CMS Physics Analysis Summary

Contact: cms-pag-conveners-b2g@cern.ch 2014/06/02

Search for Displaced Supersymmetry in Dilepton Final States

The CMS Collaboration

Abstract

We present a search for new physics producing lepton pairs whose trajectories are displaced from the interaction region. This search uses a data sample obtained from pp collisions at $\sqrt{s} = 8\,\text{TeV}$, with an integrated luminosity of $19.7\,\text{fb}^{-1}$, recorded by the CMS detector at the LHC. Many models of new physics predict particles with lifetimes on the scale that would produce detectable displacements of the decay products on the order of $100\,\mu$m-2 cm. We target a particular model called "Displaced Supersymmetry" but have designed the search to remain sensitive to a wide variety of such theoretical scenarios. The number of observed events is in agreement with the background expectation, and limits are placed on the pair production of stop squarks decaying to final states including an electron and muon, for a range of stop lifetimes between $100\,\mu\text{m}/c$ and $10\,\text{cm}/c$. At a mean stop lifetime of $2\,\text{cm}/c$ — the value that gives the highest mass exclusion — stop squarks with masses below 790 GeV are excluded at 95% confidence level.

1 Introduction and theoretical motivation

Although the standard model (SM) has proven extremely successful at describing elementary particles and their interactions, it is known to be incomplete. Experiments at the Tevatron and the Large Hadron Collider (LHC) have conducted broad programs of searches aimed at discovering or ruling out a variety of extensions to the SM which seek to make it a more complete theory. The vast majority of these searches make the assumption that new particles will have short enough lifetimes that their decay products will originate directly from the interaction region. To date, none of these searches has succeeded in finding evidence for new physics beyond the standard model (BSM).

As many of these BSM models become more and more constrained, the motivation to search for new physics with displaced signatures continues to increase. Both the CMS and ATLAS collaborations have performed searches for decays of BSM particles with long lifetimes, covering a large range of decay lengths. These range from searches for BSM particles that travel through the majority of the detector before decaying [1, 2], to BSM particles decaying within the tracking volume [3], to searches for relatively prompt signatures. The searches focusing on shorter decay lengths include hadronic [4], semileptonic [5], and dileptonic [6] final states. This search differs from the previous searches for long-lived signatures in two respects. This search is optimized to the phase space just beyond the sensitivity of prompt searches but before that of prior searches for long-lived BSM signatures. This search is also the first to dispense with the usual requirement that the displaced final state particles originate from a common vertex.

This search is designed to be as model-independent as possible and to be sensitive to as many event topologies as possible. Consequently, the event selection focuses exclusively on a displaced, isolated dilepton signature and does not try to identify signal events using hadronic activity or missing transverse momentum ($\not\!\!E_T$). In this way, we retain sensitivity to any model that can produce leptons with displacements on the order of 100 μm to 2 cm, regardless of whether these leptons are accompanied by jets, $\not\!\!E_T$, or other interesting kinematic features. Also, by removing the vertex constraint on the selected particles, we broaden the sensitivity to models containing either one or two long-lived particles per event.

We interpret the search results in the context of the Displaced Supersymmetry [7] model. This model introduces R-parity violating terms in the superpotential of the minimally supersymmetric standard model. R-parity violation (RPV) allows the lightest supersymmetric particle (LSP) to decay into SM particles. This can frustrate standard SUSY searches by lessening or removing the $\not\!\!E_T$ signature generally present in SUSY topologies. Only lepton-number-violating operators are considered in order to avoid constraints from proton decay. Due to sufficiently small couplings for these operators, the LSP will have a long enough lifetime that its decay products are measurably displaced from the region of beam-beam overlap in which the proton-proton interactions occur (henceforth referred to as the "luminous region"). For a range of these couplings, Displaced Supersymmetry can generate a natural SUSY model that could have easily escaped detection thus far at the LHC, because the displacement of the decay products will be in the gap of sensitivity between the previous searches based on prompt decays and those based on very long-lived BSM signatures.

We focus on the case in which the LSP is the stop quark — the superpartner of the top quark. At the LHC, stop squarks would be dominantly produced in pairs. The stops then decay through an RPV vertex, $\widetilde{\mathrm{t}}_1 \to \mathrm{bl}$, where l is an electron, muon, or tau lepton. To reduce dependancy on any specific model, we assume lepton universality in the stop decay vertex, so that the branching fraction to any lepton flavor is equal to one third. We conduct a search for stop decays in which there is an electron and a muon in the final state, with both of the leptons being displaced from

the luminous region.

2 Data and Monte Carlo simulation samples

This analysis uses pp collision data taken in 2012 at $\sqrt{s} = 8$ TeV, corresponding to an integrated luminosity of 19.7 $\pm$ 0.5 fb^{-1}. The events in the search sample are collected by a trigger that requires a muon with its momentum's component perpendicular to the beam axis, p_{T}, above 22 GeV. It also requires a cluster in the electromagnetic calorimeter with the transverse energy, E_{T}, above 22 GeV with no requirement for a track to point to this cluster.

We use Monte Carlo (MC) simulation for estimating our signal acceptance and for estimating contributions from $Z\to\tau\tau$, one of the two main backgrounds. The other main background is QCD, which is estimated by a data-driven method described below. Additionally, smaller sources of background, such as $t\bar{t}$, are taken from simulation. The samples simulating Z+jets and single-top-quark production were generated using POWHEG [8], while those simulating W+jets and $t\bar{t}$ were generated using MADGRAPH5 with PYTHIA6 for hadronization [9, 10]. Samples of QCD multijet production, which were used to validate our data-driven QCD background estimate, and samples of double-boson production were simulated with PYTHIA6. For the background MC samples generated with POWHEG, the `CT10` parton distribution function (PDF) is used [11]; all other samples use `CTEQ6L1` [12]. All generated events are processed through a detailed simulation of the CMS detector based on GEANT4 [13]. In figures, the samples listed above are combined for presentational clarity. The "Top" sample is the combination of $t\bar{t}$ and single top processes and the "Other EWK" sample is the combination of $Z\to ee$, $Z\to\mu\mu$, and the various diboson processes. In all figures, the "QCD" sample is obtained directly from the data.

Simulated samples of the process $pp\to\tilde{t}_1\tilde{t}_1^*$ were generated using PYTHIA8 with the `Tune4C` parameter tune and the `CTEQ6L1` PDF. The requisite samples were generated to allow us to scan over two signal parameters. First, we generate samples with stop masses from 200 GeV to 1 TeV. Second, we generate samples with stop lifetimes between 0.1 cm/c and 10 m/c. Starting with a SUSY Les Houches Accord (SLHA) file [14] corresponding to Snowmass Points and Slopes (SPS) point 1a, the mass and width of the lightest stop were modified according to the sample being produced [15].

3 Event selection

The event selections in this analysis can be grouped into two stages. First, we isolate events with exactly one electron and exactly one muon in the final state. Both the electron and muon are required to be well-reconstructed and isolated, and the two leptons are required to have opposite charge. This stage will subsequently be referred to as the analysis "preselection". The second stage involves classifying the events passing the preselection according to how far the selected leptons' trajectories are offset from the luminous region of the event.

3.1 Preselection

The preselection requirements aim at selecting events which consist of two well identified leptons, specifically one electron and one muon. The leptons are reconstructed using the particle-flow event reconstruction algorithm [16], which combines information from all the CMS subdetectors in order to reconstruct all stable particles and determine their type, momentum direction and energy.

To account for the acceptance of the CMS detector, we require an electron and a muon with $|\eta| < 2.5$, where the pseudorapidity $\eta \equiv -\ln\tan(\theta/2)$ and θ is the polar angle of the leptons' momentum vectors with respect to the counterclockwise beam. Additionally, electron candidates are vetoed if they fall within a region of low detector acceptance corresponding to $1.444 < |\eta| < 1.566$. To ensure we are operating well above the momentum thresholds required at the trigger level, we require the leptons in the event to have a transverse momentum greater than 25 GeV.

Electron candidates are reconstructed by combining information from deposits in the electromagnetic calorimeter (ECAL) and tracks built by the Gaussian sum filter (GSF) algorithm [17]. The identification of the electrons is performed using a boosted decision tree (BDT) that combines information from tracking and shower-shape observables as well as observables related to the geometrical and kinematic matching of the electron track to its supercluster. Electron isolation is achieved using a particle-flow based isolation variable. The variable is defined as the scalar sum of the transverse momenta of the particle-flow candidates, excluding the electron, within a cone of $\Delta R \equiv \sqrt{(\Delta\eta)^2 + (\Delta\phi)^2} < 0.3$ around the electron, where ϕ is the azimuthal angle in the plane transverse to the beams. The neutral component of the isolation is additionally corrected for pileup using the FastJet [18, 19] energy density (ρ) of the pileup in the event. After that correction, the isolation is almost independent of the number of vertices. We require this isolation sum to be less than 10% of the electron's p_{T}.

Muon candidates are built by separately constructing a track from the muon's path through the tracking volume and one from its path through the muon systems, and then performing a global fit between the two [20]. Similar to the electron case, muon isolation is performed by a particle-flow algorithm but with a cone of $\Delta R < 0.4$. In addition, the pileup correction is performed using a different algorithm ($\Delta\beta$) that gives an estimation of the pileup contribution on an event-by-event basis [21]. The muon isolation is required to be less than 12% of the muon's p_{T}.

Jets are constructed using the implementation of the anti-k_{T} clustering algorithm available in FastJet with a size parameter of $R = 0.5$ [22]. The input to the algorithm is the collection of all particles identified by particle-flow, but excluding electron and muon candidates. The jets used in this analysis are required to have $p_{\mathrm{T}} > 10$ GeV.

The isolation sums described above are calculated considering only the tracks associated with the most energetic vertex in the event. In rare cases, one or both of the selected leptons come from an interaction other than the one corresponding to the most energetic vertex. In such events, leptons from semi-leptonic B and D decays can pass the standard isolation cuts. Consequently, we also veto events in which either selected lepton is inside a reconstructed jet. Specifically we require that there is no reconstructed jet above 10 GeV within $\Delta R < 0.5$ of either selected lepton.

Each event is required to have exactly one electron and one muon passing all the criteria above. In these events, the two leptons are required to be separated by more than 0.5 in $\eta - \phi$ space and be oppositely charged.

The events passing the preselection are further catagorized by using the 2D track impact parameter of the selected leptons in the plane transverse to the beams. This transverse impact parameter (d_0) is defined as the distance of closest approach in the transverse plane of the helical trajectory of the lepton track to the center of the luminous region. When an unstable particle decays to charged particles, the impact parameters of these decay products will be strongly correlated with the original particle's lifetime. We exploit this fact to construct regions of phase

space that select particles from the decays of long-lived parents.

As part of the event preselection, we require that both selected leptons have $|d_0| > 100\,\mu$m. This requirement is designed to exclude sources of promptly-decaying particles; namely W and Z bosons and top quarks. The events that populate this region are primarily leptons from the $Z\to\tau\tau$ process and from heavy flavor QCD decays. This region is used to perform a data-driven estimate of the background from heavy flavor QCD decays. The procedure for this estimate is described in detail in Section 5. Finally, the selected leptons are required to have $|d_0| < 2\,$cm, in order to constrain our search sample to the leptons that fall within the requirements imposed at the triggering and reconstruction levels.

3.2 Signal search regions

By requiring both the electron and the muon in the events passing the preselection to have large enough impact parameters, we can construct a region that is largely free of leptons from promptly-decaying SM particles. However, the efficiency for a lepton to pass a given d_0 cut is directly related to the lifetime of its parent particle. Consequently, a given d_0 cut will have drastically different efficiencies at different values of the parent particle lifetime. In order to optimize the selection criteria for a wide range of parent particle lifetime, we construct three signal regions — optimized to different lifetimes — and use them simultaneously in the limit-setting procedure. The three signal regions are defined in the two-dimensional space of electron $|d_0|$ and muon $|d_0|$. The most exclusive region, requiring (for both the electron and the muon) $|d_0| > 1000\,\mu$m, is expected to have very low background contamination. Events enter the intermediate signal region if the event fails the cuts defining the most exclusive region, but both leptons have $|d_0| > 500\,\mu$m. Similarly, an event enters the loose signal region if it fails to enter the intermediate one, but both leptons have $|d_0| > 200\,\mu$m. This loose signal region is expected to contain more background contamination, but retain higher signal efficiency for the shortest stop lifetimes we consider. These regions are purposely constructed such that there is no overlap between them so that they can be used in combination when setting limits.

4 Corrections to the Monte Carlo simulations

In order to account for known differences in the behavior of simulation and data, we apply a series of corrective factors to the simulation. This section details the methods used in the determination and application of these corrections.

4.1 Event pileup reweighting

The simulated samples are generated with a distribution of number of interactions that approximates the projections for the future LHC conditions. At the end of the data-taking period, the simulation is reweighted using the true distribution of the number of inelastic interactions in data. The reweighting factors are calculated independently for each simulated dataset, by dividing the data and simulation in each bin of number of interactions.

4.2 Lepton reconstruction and identification corrections

Scale factors are derived to account for differences in the performance of lepton identification and isolation algorithms between data and simulation. The lepton corrections are estimated with the tag and probe method [23] using the $Z\to ll$ process. The MC events are reweighted according to the data/MC scale factors per lepton, as a function of their p_T and $|\eta|$. The lepton scale factors are estimated exclusively for this analysis in order to make sure any d_0 and d_z

requirements which are included in the CMS official efficiency estimation are removed. These corrections are not designed to account for the behavior of very displaced leptons, since the Z boson decays promptly. Instead, we use these corrections as a baseline and use several other control samples to verify the modeling of displaced leptons.

In order to verify that the simulation is reliable for leptons with large impact parameters, we look at the events in which one of the leptons is prompt and the other is allowed to be either prompt or displaced. In this way, we construct a background-dominated region, with a large number of non-prompt leptons populating it, which does not overlap with any signal region. This allows us to compare data and simulation into the tails of the impact parameter spectra. Two regions are defined - one for electrons and one for muons. For each region, the prompt lepton is required to have $|d_0| < 200\,\mu$m and the other lepton is required to have $|d_0| > 100\,\mu$m. Figure 1 shows the impact parameter distributions of the leptons in the region which contains another prompt lepton with opposite flavor. In this figure, the QCD contribution is estimated using the data, scaling the events in the anti-isolated region to match the yields in the isolated region as those regions are defined in section 5. Here we see evidence that the shape of the data is well modeled by the simulation, even into the tails of the $|d_0|$ distributions.

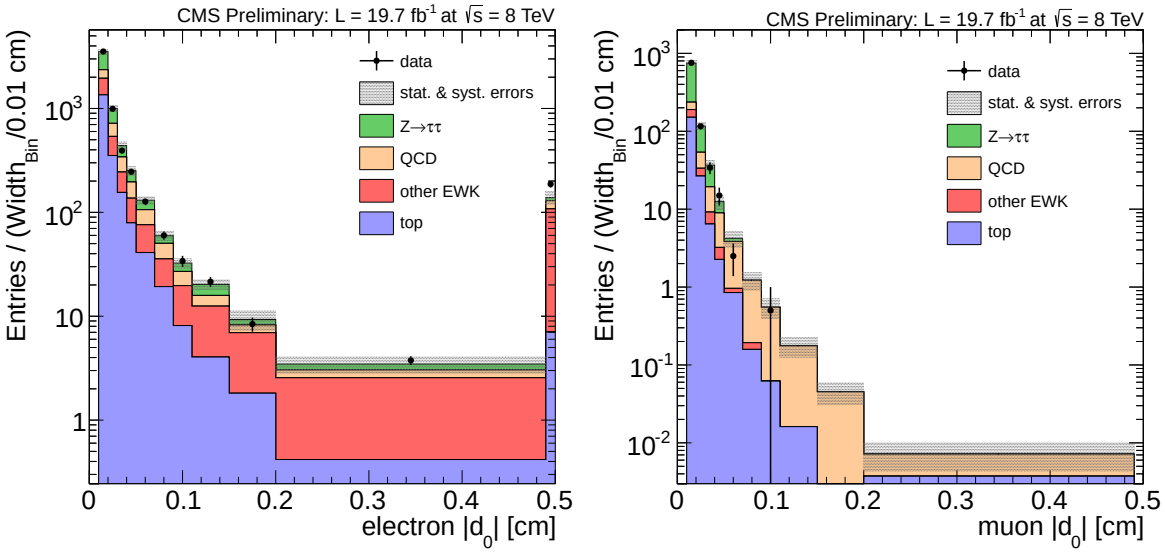

Figure 1: Lepton transverse impact parameter spectra in the region which contains another prompt lepton with opposite flavor, for electrons (left) and muons (right). The bin contents have been rescaled to account for the varying sizes of the bins. The contents of the overflow bin are added to the rightmost bin of the plot.

To estimate the degradation of lepton track reconstruction at high impact parameter, we use dedicated samples of cosmic muon events in data and MC. Up to a $|d_0|$ of 2 cm, the tracking efficiency is above 90% for both data and MC. We use these events to calculate a scale factor to correct for the difference between data and MC in the region in which $|d_0| > 200\,\mu$m. This scale factor is measured to be 0.960 ± 0.014, where the uncertainty comes from the limited statistics of the samples. This factor is applied to leptons in the simulated events passing the analysis selections. A similar method of deriving such scale factors can be found in [6].

4.3 Trigger efficiency corrections

Trigger efficiencies are estimated using a data sample collected with jet/MET triggers, which are uncorrelated with our event selections. This sample is enriched with $\bar{t}t$ events by requiring

the preselected events from this sample to have an electron and a muon candidate, two jets with $p_T > 30$ GeV and $|\eta| < 2.4$, and at least one b-jet, selected with the medium working point of the combined secondary vertex (CSV) algorithm [24]. This $t\bar{t}$ enriched sample has negligible QCD background.

The trigger scale factor is defined as the ratio of $\epsilon_{Data}^{MET/jet}/\epsilon_{MC}^{t\bar{t}}$ after applying the preselection requirements. The numerator is calculated by the number of MET/jet events passing the HLT_Mu22_Photon22_CaloIdL trigger over the total number of events which pass the orthogonal MET/jet trigger. The denominator is calculated in a similar way using $t\bar{t}$ events. The final scale factor is estimated to be 0.981 +/- 0.004. This number is eventually used to correct the MC in order to match the data and the statistical error is obtained by a simple error propagation.

5 Background estimation techniques

There are two main sources of leptons with the range of displacements in which this search focuses. These come from the two types of particles with leptonic decays that have lifetimes in the range of interest: heavy flavor QCD, such as B and D mesons ($\tau \approx 500\,\mu$m$/c$), and tau leptons ($\tau \approx 87\,\mu$m$/c$). Consequently, the two primary backgrounds to this search are from semileptonic, heavy-flavor QCD decays (henceforth referred to as QCD) and the $Z\to\tau\tau$ process where each tau lepton decays leptonically. Since the cross sections for most QCD processes are so large, the simulated QCD samples are not sufficiently large to describe this background. Therefore, the expectation for this background is derived from the data. The background expectation for the $Z\to\tau\tau$ process is taken from simulation, after validating that the simulated dataset can accurately reproduce the behavior of $Z\to\tau\tau$ events in data, especially in the case in which the leptons are displaced. Other, less significant backgrounds come from $t\bar{t}$, single top, diboson, and $(W\to l\nu)$+jets processes, and are taken directly from the simulation.

The QCD estimate is calculated using the events passing all of the analysis preselections. In this data-driven estimation, we apply a methodology in which we use two uncorrelated variables to define four non-overlapping regions. The method then calculates the ratio of events in two of the regions and applies it to the number of events in a third region to predict the number of events in the fourth region. The uncorrelated variables we use are the leptons' isolation requirements and the signs of the leptons' charges. With these variables, we can define the following four regions: isolated leptons whose charges have the opposite sign (OS); isolated leptons whose charges have the same sign (SS); anti-isolated, OS leptons; and anti-isolated, SS leptons. The region of isolated, OS leptons corresponds to the normal analysis preselection, while the other three regions are expected to contain primarily QCD multijet events. Any contribution from other sources in these three regions is taken from simulation and subtracted when performing the QCD estimate. When looking into the regions with anti-isolated leptons, instead of simply inverting the isolation requirements for both leptons we define an isolation sideband region. Where the normal isolation requirements are $\text{iso}_e < 0.1$ and $\text{iso}_\mu < 0.12$, the isolation sideband is defined as $0.2 < \text{iso}_e < 1$ and $0.24 < \text{iso}_\mu < 1.5$. This sideband approach has two advantages over a simple cut inversion. First, it allows us to put some separation between the isolated and anti-isolated regions, ensuring the anti-isolated sideband will contain negligible amounts of non-QCD events. Secondly, we can choose not to include events in the high tails of the lepton isolation spectra, which are generally less well understood. In addition to altering the requirements on the lepton isolation sums, the requirement that the lepton not be close to a jet ($\Delta R_{l,\text{jet}} > 0.5$) is removed when defining the anti-isolated regions.

We calculate a scale factor as the ratio of the number of QCD events in the region of *isolated* SS

leptons to the number of QCD events in the region of *anti-isolated* SS leptons. In each region we take the QCD contribution to be the difference of data and non-QCD simulation. We then construct a data-derived QCD dataset by taking the events in the region of anti-isolated OS leptons and normalizing them to the region of isolated OS leptons using this scale factor. We can then use the impact parameter spectra from this QCD dataset to apply the additional $|d_0|$ selections and obtain the QCD expectation in the signal regions. In order to verify that the lepton impact parameter spectra are uncorrelated with the lepton isolation spectra, we compare the $|d_0|$ distributions for isolated and anti-isolated leptons, in a dedicated control sample in the data that is enriched in heavy flavor QCD decays.

The other dominant source of background is the $Z\to\tau\tau$ process. We use the simulation to describe this process, but we verify its effectiveness in a dedicated control region. This control region is defined by applying the analysis preselection, without any requirements on lepton impact parameter, and then a series of $Z\to\tau\tau$-enriching selections. These cuts are designed to reject other sources of SM background as well as any possible events from the signal process. In order to reject $(W\to l\nu)$+jets events, for both leptons, we require that mass of the lepton plus missing energy system be less than 50 GeV. To reject QCD and $t\bar{t}$ events, we require the total scalar sum of transverse jet energy to be less than 100 GeV. Finally, since the $Z\to\tau\tau$ process preferentially produces leptons that are back-to-back in ϕ, we require the two leptons to be separated in ϕ by more than 2.5. This also helps reject signal events, in which the leptons are generally isotropically distributed in ϕ. We verify that the simulated sample has enough events to describe the tails of the lepton impact parameter distributions with adequate statistical precision. We also use this control region to demonstrate that the shapes of the lepton impact parameter spectra in data are well-modeled by the simulation. Figure 2 shows the lepton impact parameter spectra in this $Z\to\tau\tau$ control region, for data and simulation. A good agreement between the distributions in data and simulation for this process at high $|d_0|$ justifies using the simulation to extract the $Z\to\tau\tau$ background estimate.

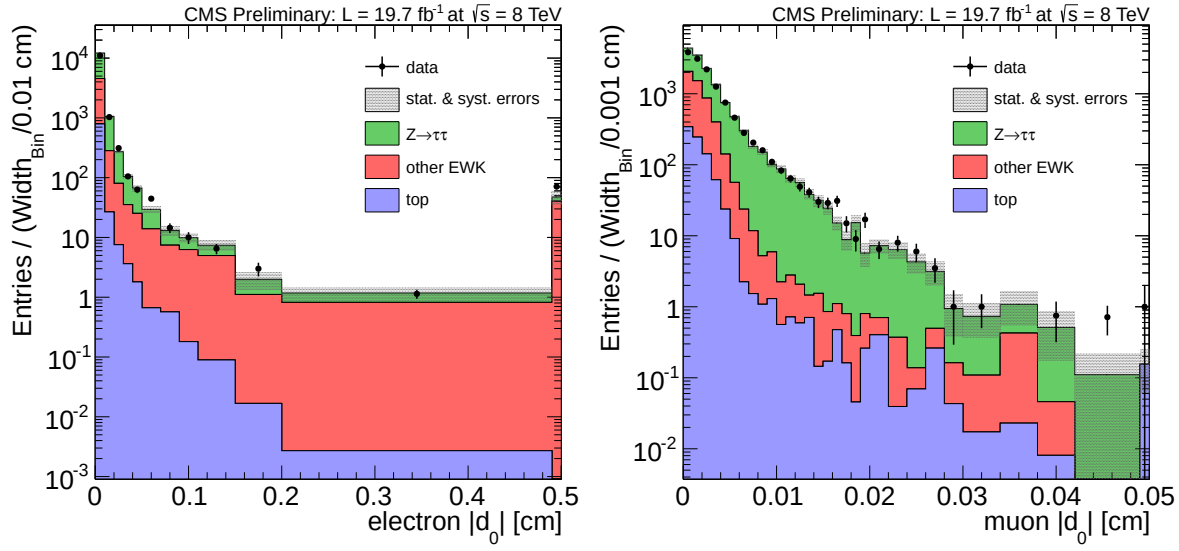

Figure 2: Lepton transverse impact parameter spectra of electrons (left) and muons (right) in $Z\to\tau\tau$ control region, up to 5000 μm and 500 μm, respectively. The bin contents have been rescaled to account for the varying sizes of the bins. The contents of the overflow bin are added to the rightmost bin of the plot.

Before applying the additional requirements on $|d_0|$ that define our signal regions, we verify

that the background estimations accurately reproduce the behavior of the data with the preselection criteria applied. Table 1 shows the expected and observed numbers of events passing all preselection requirements. The systematic uncertainties quoted on these yields are those derived in Section 6. Good agreement is seen between the background expectation and observation in terms of the number of events. Since requirements will be placed on the lepton impact parameters, we want to additionally verify that the background estimate correctly describes the shape of these quantities. Figure 3 shows the $|d_0|$ spectra for background and data. Again, good agreement is seen between data and the background expectation.

Table 1: Numbers of expected and observed events that pass the preselection requirements.

Event Source	Event Yield $\pm$ 1σ (stat.) $\pm$ 1σ (syst.)
other EWK	$3.56 \pm 0.99 \pm 0.43$
top	$10.3 \pm 1.0 \pm 0.8$
QCD	$50 \pm 0.01 \pm 15$
$Z \to \tau\tau$	$98.2 \pm 9.2 \pm 8.0$
Total expected background	$162 \pm 9 \pm 17$
Observation	154

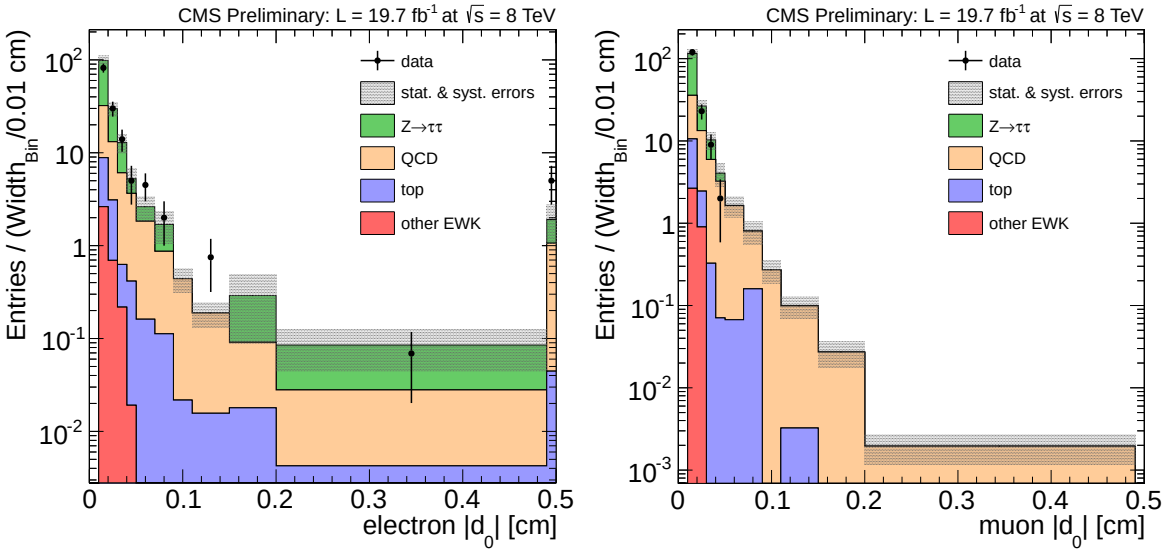

Figure 3: Lepton transverse impact parameter spectra of the sum of background expectations after the preselection requirements, for electrons (left) and muons (right). The bin contents have been rescaled to account for the varying sizes of the bins. The contents of the overflow bin are added to the rightmost bin of the plot.

We want now to compare the event yield between our background and the data in the signal regions. Since these regions require a high $|d_0|$ for the muon and the electron simultaneously, we expect very small contributions from all background sources. Often, the efficiency for a background process is less than the efficiency to give one unweighted MC event, in which case the raw MC expectation is zero events. In order to avoid this, we use a different method to estimate the background for high $|d_0|$. For each background, we calculate separately the efficiency to pass the $|d_0|$ cut for the selected electron and the selected muon. Then we estimate the number of events that pass both cuts by multiplying the two efficiencies together and applying this event-level efficiency to the events passing the preselection. Using this factorised

approach, we reduce the statistic error on the estimate and limit the cases in which the expected yield for a given background is null. In the cases in which the factorised approach gives a null estimate, we use the yield from the less exclusive neighboring signal region, which should be a conservative upper limit.

6 Systematic uncertainties

There are several sources of systematic uncertainty relevant to this analysis. These sources include uncertainties on the MC correction factors, such as the lepton efficiency scale factors and the trigger efficiency scale factors. There are also uncertainties associated with the modelling of pileup in the simulation, the integrated luminosity, the QCD background estimation, and the cross sections of the different MC samples. In addition, theory uncertainties arising from the PDF sets are also calculated.

The uncertainty on the lepton efficiency has been computed by varying each correction factor used for the rescaling by $\pm\sigma$ and then quoting the effect on the final yields.

The systematic uncertainty associated with the trigger efficiency was conservatively evaluated to be the difference between the data/MC scale factor and unity, on the order of 2% .

For the displaced track reconstruction efficiency correction, the full size of the correction (4%) is taken as a systematic uncertainty on each lepton. Since each event contains two leptons, this corresponds to a 5.7% uncertainty per event.

The estimation of the luminosity for the 2012 pp run is based on the pixel cluster counting method [25]. This method yielded a new CMS recommended luminosity estimation with an uncertainty of 2.6% for the 8 TeV dataset which is used in the analysis.

For samples generated using MADGRAPH with PYTHIA6 for hadronization ($(W\to l\nu)$+jets and $t\bar{t}$), QCD scale and matching uncertainties are evaluated using dedicated simulation to evaluate the effect of $\pm1\sigma$ fluctuations about the default values used in the standard simulation. For the $(W\to l\nu)$+jets sample, the scale uncertainty is $\pm$2.6% and the matching uncertainty is $\pm$8%. For the $t\bar{t}$ sample, the scale uncertainty is $\pm$2% and the matching uncertainty is $\pm$0.4%. Since the other simulated samples are produced with a single generator, such uncertainties do not apply to them.

The systematic uncertainties on the QCD background estimate is obtained by propagating the statistical error on the data used, as well as the statistical and systematic uncertainties on the simulation used. It is driven by the statistical and systematic errors in the region of isolated, SS leptons and is calculated to be 30%.

Cross sections and their uncertainties are all taken from theoretical calculations. The uncertainty on the $(W\to l\nu)$+jets and $Z\to ll$ processes is taken from an NNLO calculation with FEWZ 3.1 [26]. The uncertainty on diboson processes is cited from a previous CMS result[27]. The uncertainty on single top processes is taken from the approximate NLO calculation in [28]. The uncertainty on the $t\bar{t}$ process is quoted from the NNLO calulation in [29]. The uncertainty on stop pair production is taken from the NLO+NLL calculation in [30–32].

In order to estimate the uncertainty due to pileup events we vary the number of interactions in the simulation ($\pm$ 3.9% for 2012) and note the changes on the selection yields. The pileup reweighting is done by generating target pileup distributions with the inelastic pp cross section shifted by $\pm\sigma$. The central value for the total inelastic cross section used for 2012 is 69.4 mb.

Systematic uncertainties associated with the parton distribution functions are provided by the PDF builders and can be accessed via the LHAPDF (Les Houches Accord Parton Distribution Function) library [33, 34]. Following the official PDF4LHC recommendation [35] we estimated the acceptance uncertainties using the PDF re-weighting method. According to the PDF4LHC recipe the systematic errors are obtained by the use of an envelope of the CTEQ, MSTW and NNPDF PDF sets.

The systematic uncertainties on simulated samples used in this analysis are summarized in Table 2. Uncertainties that have the same value for all processes and those that only apply to certain samples are not individually listed in the table. The values quoted for the signal simulation show the range of uncertainties over all choices of signal model parameters. Uncertainties for the signal process generally increase with the stop mass, and remain relatively constant as a function of stop lifetime. The rightmost column shows the total systematic uncertainty on each sample, incorporating both the other columns in the table as well as other uncertainties described in this section.

Table 2: Sources of systematic uncertainty relevant to this search. The rightmost column includes all the relevant systematic uncertainties, not only those explicitly mentioned in the table.

Dataset	Cross-section	Pileup	e ID/ISO	μ ID/ISO	PDF	Total
W$\to$lν	$\pm$3.5%	$\pm$0.07%	$\pm$0.42%	$\pm$0.61%	$\pm$0.66%	$\pm$11.0%
diboson	$\pm$6.2%	$\pm$0.28%	$\pm$0.35%	$\pm$0.63%	$\pm$0.59%	$\pm$9.0%
single top	$\pm$6.9%	$\pm$0.17%	$\pm$0.29%	$\pm$0.64%	$\pm$2.15%	$\pm$9.4%
$t\bar{t}$	$\pm$4.3%	$\pm$0.19%	$\pm$0.49%	$\pm$0.56%	$\pm$0.11%	$\pm$8.0%
Z$\to$ll	$\pm$4.6%	$\pm$0.21%	$\pm$0.29%	$\pm$0.64%	$\pm$1.66%	$\pm$8.1%
QCD	—	—	—	—	—	$\pm$30%
signal	$\pm$15-28%	$\pm$0.1-5.4%	$\pm$0.13-0.29%	$\pm$0.9-3.8%	$\pm$0.06-4.6%	$\pm$15-28%

7 Results

Table 3 shows the numbers of expected background events in our search regions, as well as the observation. Only leptons with $|d_0| < 2\,\text{cm}$ are included in the search regions. In the case in which zero events are predicted, we take the estimate from the previous search region with a non-zero expected background yield. We denote this with a preceding "$<$" to indicate that this is a conservative estimate.

Since we do not observe any significant excess over the background expectation, we set 95% CL upper limits on the cross section for stop pair production at 8 TeV. This is done with a Bayesian calculation with flat priors for the signal strength. These are then converted into upper limits on the mass of the stop, where the cross section for each mass hypothesis is calculated at NLO+NLL precision within a simplified model with decoupled squarks and gluinos [30–32]. We do this for each stop lifetime hypothesis that we consider. The resulting expected and observed limit contours are shown in Figure 4 with the region to the left of the contours being excluded. We are able to exclude stop masses up to 790 GeV for a lifetime of $2\,\text{cm}/c$.

Table 3: Numbers of expected and observed events in the three search regions. Background and signal expectations are quoted as $N_{exp} \pm \sigma(\text{stat.}) \pm \sigma(\text{syst.})$. When the raw estimate of a background is null in some search region, the estimate is instead taken from the preceding region. Since this should strictly overestimate the background, we denote this by a preceding "$<$".

Event Source	0.02 cm $< \lvert d_0 \rvert <$ 0.05 cm	0.05 cm $< \lvert d_0 \rvert <$ 0.1 cm	$\lvert d_0 \rvert >$ 0.1 cm
other EWK	$0.65 \pm 0.13 \pm 0.08$	$(0.89 \pm 0.53 \pm 0.11) \times 10^{-2}$	$<(89 \pm 53 \pm 11) \times 10^{-4}$
top	$0.767 \pm 0.038 \pm 0.061$	$(1.25 \pm 0.26 \pm 0.10) \times 10^{-2}$	$(2.4 \pm 1.3 \pm 0.2) \times 10^{-4}$
Z$\to\tau\tau$	$3.93 \pm 0.42 \pm 0.32$	$(0.73 \pm 0.73 \pm 0.06) \times 10^{-2}$	$<(73 \pm 73 \pm 6) \times 10^{-4}$
QCD	$12.7 \pm 0.2 \pm 3.8$	$(98 \pm 6 \pm 30) \times 10^{-2}$	$(340 \pm 110 \pm 100) \times 10^{-4}$
Total expected background	$18.0 \pm 0.5 \pm 3.8$	$1.01 \pm 0.06 \pm 0.30$	$0.051 \pm 0.015 \pm 0.010$
Observation	19	0	0
$pp\to\tilde{t}_1\tilde{t}_1^*$			
M = 500 GeV, $\langle c\tau \rangle$ = 1 mm	$30.1 \pm 0.7 \pm 1.1$	$6.54 \pm 0.34 \pm 0.24$	$1.34 \pm 0.15 \pm 0.05$
M = 500 GeV, $\langle c\tau \rangle$ = 1 cm	$35.3 \pm 0.8 \pm 1.3$	$30.3 \pm 0.7 \pm 1.1$	$51.3 \pm 1.0 \pm 1.9$
M = 500 GeV, $\langle c\tau \rangle$ = 10 cm	$4.73 \pm 0.30 \pm 0.17$	$5.57 \pm 0.32 \pm 0.20$	$26.27 \pm 0.70 \pm 0.93$

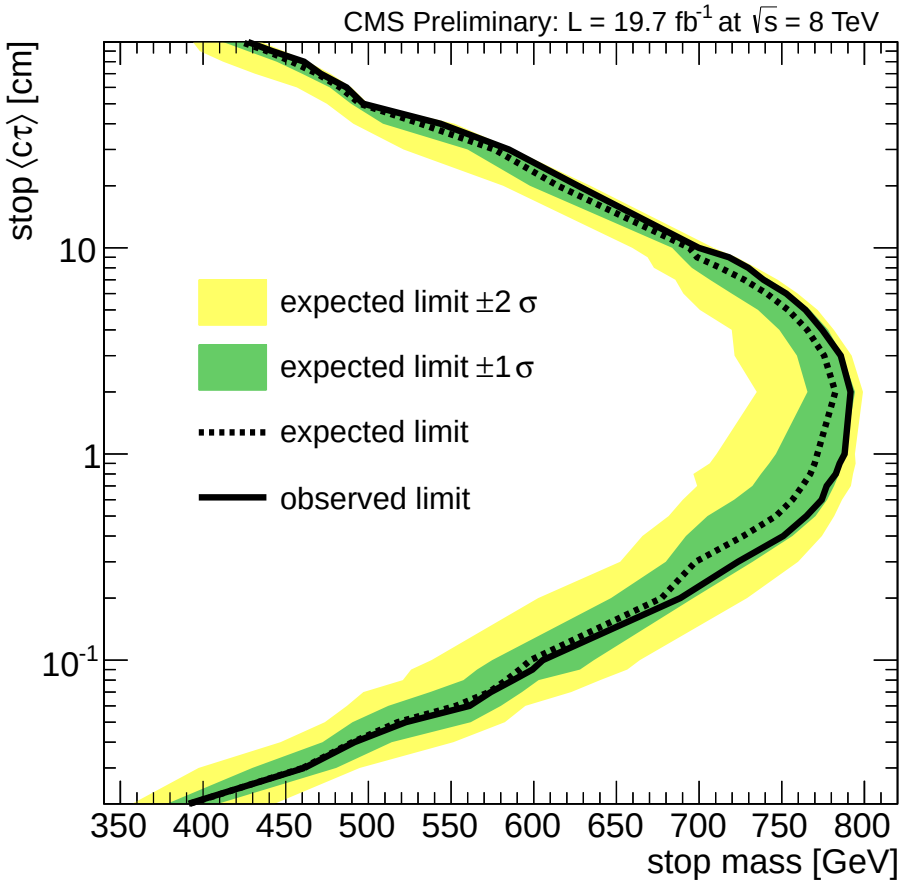

Figure 4: Expected and observed 95% CL exclusion contours for stop pair production in the plane of stop $\langle c\tau \rangle$ and mass. The region to the left of the contours is excluded by this search.

8 Conclusion

In summary, a search has been performed for new physics with an electron and muon in the final state which are displaced transversely from the LHC luminous region, with no requirements made on jets or missing energy. The data sample corresponds to 19.7 fb^{-1} of proton-proton collisions recorded by the CMS detector at the LHC during the 2012 run at $\sqrt{s} = 8\,\text{TeV}$. No excess is observed above the estimated number of background events for displacements up to 2 cm. The results are interpreted in the context of a "displaced supersymmetry" model with a pair-produced stop LSP having a lifetime up to 1 m/c. We place limits at 95% CL on this model as a function of stop mass and stop lifetime. For a lifetime hypothesis of 2 cm/c, we exclude stops up to 790 GeV in mass.

References

[1] CMS Collaboration, "Search for heavy long-lived charged particles in pp collisions at $\sqrt{s} = 7\,\text{TeV}$", *Phys. Lett. B* **713** (2012) 408–433, doi:10.1016/j.physletb.2012.06.023, arXiv:1205.0272.

[2] ATLAS Collaboration, "Searches for heavy long-lived sleptons and R-hadrons with the ATLAS detector in pp collisions at $\sqrt{s} = 7\,\text{TeV}$", *Phys. Lett. B* **720** (2013) 277–308, doi:10.1016/j.physletb.2013.02.015, arXiv:1211.1597.

[3] ATLAS Collaboration, "Search for direct chargino production in anomaly-mediated supersymmetry breaking models based on a disappearing-track signature in pp collisions at $\sqrt{s} = 7\,\text{TeV}$ with the ATLAS detector", *JHEP* **1301** (2013) 131, doi:10.1007/JHEP01(2013)131, arXiv:1210.2852.

[4] ATLAS Collaboration, "Search for displaced vertices arising from decays of new heavy particles in 7 TeV pp collisions at ATLAS", *Phys. Lett. B* **707** (2012) 478–496, doi:10.1016/j.physletb.2011.12.057, arXiv:1109.2242.

[5] ATLAS Collaboration, "Search for long-lived, heavy particles in final states with a muon and multi-track displaced vertex in proton-proton collisions at $\sqrt{s} = 7\,\text{TeV}$ with the ATLAS detector", *Phys. Lett. B* **719** (2013) 280–298, doi:10.1016/j.physletb.2013.01.042, arXiv:1210.7451.

[6] CMS Collaboration, "Search in leptonic channels for heavy resonances decaying to long-lived neutral particles", *JHEP* **1302** (2013) 085, doi:10.1007/JHEP02(2013)085, arXiv:1211.2472.

[7] P. W. Graham, D. E. Kaplan, S. Rajendran, and P. Saraswat, "Displaced supersymmetry", *JHEP* **1207** (2012) 149, doi:10.1007/JHEP07(2012)149, arXiv:1204.6038.

[8] S. Frixione, P. Nason, and C. Oleari, "Matching NLO QCD computations with parton shower simulations: the POWHEG method", *JHEP* **0711** (2007) 070, doi:10.1088/1126-6708/2007/11/070, arXiv:0709.2092.

[9] J. Alwall et al., "MadGraph 5 : going beyond", *JHEP* **1106** (2011) 128, doi:10.1007/JHEP06(2011)128, arXiv:1106.0522.

[10] T. Sjostrand, S. Mrenna, and P. Z. Skands, "PYTHIA 6.4 physics and manual", *JHEP* **0605** (2006) 026, doi:10.1088/1126-6708/2006/05/026, arXiv:hep-ph/0603175.

[11] H.-L. Lai et al., "New parton distributions for collider physics", *Phys. Rev.* **D82** (2010) 074024, doi:10.1103/PhysRevD.82.074024, arXiv:1007.2241.

[12] J. Pumplin et al., "New generation of parton distributions with uncertainties from global QCD analysis", *JHEP* **0207** (2002) 012, doi:10.1088/1126-6708/2002/07/012, arXiv:hep-ph/0201195.

[13] GEANT4 Collaboration, "GEANT4: a simulation toolkit", *Nucl. Instrum. Meth. A* **506** (2003) 250–303, doi:10.1016/S0168-9002(03)01368-8.

[14] J. Alwall et al., "A standard format for Les Houches event files", *Comput. Phys. Commun.* **176** (2007) 300–304, doi:10.1016/j.cpc.2006.11.010, arXiv:hep-ph/0609017.

[15] B. Allanach et al., "The Snowmass points and slopes: benchmarks for SUSY searches", *Eur. Phys. J. C* **25** (2002) 113–123, doi:10.1007/s10052-002-0949-3, arXiv:hep-ph/0202233.

[16] CMS Collaboration, "Particle-flow event reconstruction in CMS and performance for jets, taus, and MET", CMS Physics Analysis Summary CMS-PAS-PFT-09-001, CERN, 2009.

[17] CMS Collaboration, "Electron reconstruction and identification at $\sqrt{s} = 7$ TeV", CMS Note CMS-DP-2010-032, CERN-CMS-DP-2010-032, CERN, 2010.

[18] M. Cacciari and G. P. Salam, "Pileup subtraction using jet areas", *Phys. Lett. B* **659** (2008) 119–126, doi:10.1016/j.physletb.2007.09.077, arXiv:0707.1378.

[19] M. Cacciari, G. P. Salam, and G. Soyez, "FastJet user manual", *Eur. Phys. J.* **C72** (2012) 1896, doi:10.1140/epjc/s10052-012-1896-2, arXiv:1111.6097.

[20] CMS Collaboration, "Performance of CMS muon reconstruction in pp collision events at $\sqrt{s} = 7$ TeV", *JINST* **7** (2012) P10002, doi:10.1088/1748-0221/7/10/P10002, arXiv:1206.4071.

[21] CMS Collaboration, "Commissioning of the particle-flow reconstruction in minimum-bias and jet events from pp Collisions at 7 TeV", CMS Physics Analysis Summary CMS-PAS-PFT-10-002, CERN, 2010.

[22] M. Cacciari, G. P. Salam, and G. Soyez, "The anti-k_{T} jet clustering algorithm", *JHEP* **0804** (2008) 063, doi:10.1088/1126-6708/2008/04/063, arXiv:0802.1189.

[23] CMS Collaboration, "Measurements of inclusive W and Z cross sections in pp collisions at $\sqrt{s} = 7$ TeV", *JHEP* **1101** (2011) 080, doi:10.1007/JHEP01(2011)080, arXiv:1012.2466.

[24] CMS Collaboration, "Performance of b tagging at $\sqrt{s} = 8$ TeV in multijet, ttbar and boosted topology events", CMS Physics Analysis Summary CMS-PAS-BTV-13-001, CERN, 2013.

[25] CMS Collaboration, "CMS luminosity based on pixel cluster counting - summer 2013 update", CMS Physics Analysis Summary CMS-PAS-LUM-13-001, CERN, 2013.

[26] Y. Li and F. Petriello, "Combining QCD and electroweak corrections to dilepton production in FEWZ", *Phys. Rev.* **D86** (2012) 094034, doi:10.1103/PhysRevD.86.094034, arXiv:1208.5967.

[27] CMS Collaboration, "Measurement of W^+W^- and ZZ production cross sections in pp collisions at $\sqrt{s} = 8\,\text{TeV}$", *Phys. Lett. B* **721** (2013) 190–211, doi:10.1016/j.physletb.2013.03.027, arXiv:1301.4698.

[28] N. Kidonakis, "Differential and total cross sections for top pair and single top production", doi:10.3204/DESY-PROC-2012-02/251, arXiv:1205.3453.

[29] M. Czakon, P. Fiedler, and A. Mitov, "The total top quark pair production cross-section at hadron colliders through $O(\alpha_S^4)$", *Phys. Rev. Lett.* **110** (2013) 252004, doi:10.1103/PhysRevLett.110.252004, arXiv:1303.6254.

[30] M. Kramer et al., "Supersymmetry production cross sections in pp collisions at $\sqrt{s} = 7\,\text{TeV}$", arXiv:1206.2892.

[31] J. Alwall, P. Schuster, and N. Toro, "Simplified models for a first characterization of new physics at the LHC", *Phys. Rev. D* **79** (2009) 075020, doi:10.1103/PhysRevD.79.075020, arXiv:0810.3921.

[32] CMS Collaboration, "Interpretation of searches for supersymmetry with simplified models", *Phys. Rev. D* **88** (2013) 052017, doi:10.1103/PhysRevD.88.052017, arXiv:1301.2175.

[33] M. Whalley, D. Bourilkov, and R. Group, "The Les Houches Accord PDFs (LHAPDF) and LHAGLUE", arXiv:hep-ph/0508110.

[34] D. Bourilkov, R. C. Group, and M. R. Whalley, "LHAPDF: PDF use from the Tevatron to the LHC", arXiv:hep-ph/0605240.

[35] S. Alekhin et al., "The PDF4LHC Working Group Interim Report", arXiv:1101.0536.